Two Cytochrome P450 epoxidases mediate juvenile hormone biosynthesis in *Drosophila melanogaster*

Daiki Fujinaga[a,b], Yuya Ohhara[c,d], Naoki Okamoto[a,b,e], Hannah Chu[a,b,1], Kerry E. Mauck[a], and Naoki Yamanaka[a,b,*]

[a]Department of Entomology, University of California, Riverside, Riverside, CA 92521, USA

[b]Institute for Integrative Genome Biology, University of California, Riverside, Riverside, CA 92521, USA

[c]School of Food and Nutritional Sciences, University of Shizuoka, Suruga-ku, Shizuoka 422-8526, Japan

[d]Graduate School of Integrated Pharmaceutical and Nutritional Sciences, University of Shizuoka, Suruga-ku, Shizuoka 422-8526, Japan

[e]Life Science Center for Survival Dynamics, Tsukuba Advanced Research Alliance (TARA), University of Tsukuba, Tsukuba, Ibaraki 305-8577, Japan

[1]Present address: Department of Sciences, John Jay College of Criminal Justice - The City University of New York, New York, NY 10019, USA

*Corresponding author: Naoki Yamanaka, naoki.yamanaka@ucr.edu

Abstract

Juvenile hormones (JHs) mediate various biological processes such as development and reproduction in insects. Although pleiotropic functions of JHs are well investigated in the fruit fly *Drosophila melanogaster*, their biosynthetic mechanisms are less well understood, partly because many JH biosynthetic enzymes still remain unidentified in this important model species. Here we report that two cytochrome P450 (CYP) epoxidases mediate JH biosynthesis in *D. melanogaster*. In addition to previously reported Cyp6g2, a second epoxidase, Cyp6a13, also functions in the corpus allatum, the major JH biosynthetic endocrine gland. Combined mutations of the genes encoding these enzymes cause developmental and reproductive defects, which can be rescued by JH application. JH biosynthetic functions of these genes were further confirmed by using a heterologous expression system and *ex vivo* tissue culture. Collectively, our results indicate that these two CYP epoxidases function cooperatively to mediate JH biosynthesis in *D. melanogaster*.

37 **Highlights**

38 - *Drosophila* Cyp6g2 and Cyp6a13 are highly expressed in the corpus allatum.

39 - Combined knockout mutants of the CYP genes exhibit developmental and reproductive defects.

40 - Mutant phenotypes were rescued by feeding juvenile hormones.

41 - Both Cyp6g2 and Cyp6a13 catalyze epoxidation of juvenile hormone precursors.

42

43 Keywords

44 Juvenile hormone; *Drosophila melanogaster*; Metamorphosis; Cytochrome P450; Mass

45 spectrometry

46 **1. Introduction**

47 Juvenile hormones (JHs) are aliphatic sesquiterpenoids that regulate diverse biological
48 processes in insects, including development and reproduction (Jindra et al., 2013; Jindra and
49 Noriega, 2025). JH acts as a "status quo" hormone that maintains the juvenile form across many
50 insect orders during early postembryonic development (Riddiford, 2020), and a decline in the
51 hemolymph JH titer triggers metamorphosis (Jindra, 2019). Ablation of the corpora allata (CA),
52 the JH-producing glands, causes precocious metamorphosis, whereas ectopic application of JH
53 analogs such as methoprene induces supernumerary larval or nymphal molts in various species
54 (Konopova et al., 2011; Kayukawa et al., 2012). JH is thus considered as a key regulator that
55 prevents metamorphosis (Jindra et al., 2013). Intriguingly, JH is also produced at the onset of
56 metamorphosis in holometabolous insects (Jindra, 2019). Disruption of JH receptors causes
57 pupation defects (Konopova and Jindra, 2007; Abdou et al., 2011), suggesting that JH
58 contributes to the proper initiation of metamorphosis, potentially by preventing premature adult
59 differentiation (Martín et al., 2025).

60 The biosynthetic pathway of JH is well characterized and divided into early and late steps
61 (Bellés et al., 2005). In the early steps, known collectively as the mevalonate pathway, farnesyl
62 pyrophosphate (FPP) is synthesized. In late steps, FPP is first converted into farnesoic acid (FA)
63 by a phosphatase and reductases (Noriega, 2014). The sequence of the final JH biosynthetic steps
64 differs among insect taxa. In Lepidoptera, FA is epoxidized to JH acid (JHA) by a cytochrome
65 P450 (CYP) epoxidase and then methylated by JHA methyltransferase (Jhamt) to produce JH
66 (Daimon et al., 2012; Shinoda et al., 2003). In contrast, in most other insect orders, FA is first
67 methylated by Jhamt to form methyl farnesoate (MF), which is subsequently epoxidized to yield
68 JH (Defelipe et al., 2011). Once synthesized, JH regulates gene expression in peripheral tissues

69 by interacting with its intracellular receptor Methoprene-tolerant (Met). In the fruit fly
70 *Drosophila melanogaster*, this function is shared by its paralog, germ-cell expressed (gce)
71 (Konopova et al., 2007; Jindra et al., 2015).
72 The molecular mechanisms of JH-mediated developmental regulation have been extensively
73 investigated in *D. melanogaster* using genetic tools such as the Gal4-UAS system. Although
74 genetically allatectomized *Drosophila* larvae (also referred to as CA-ablated or CAX larvae) do
75 not undergo precocious metamorphosis, they exhibit premature differentiation of some tissues,
76 such as the eye disks and fat body (Liu et al., 2009; Riddiford et al., 2010; Zhang et al., 2022).
77 Both CAX and JH receptor knockout larvae remain viable until pupariation, but they typically
78 die around the time of head eversion, failing to complete pupation (Riddiford et al., 2010; Abdou
79 et al., 2011). In adults, JH functions as a pleiotropic hormone. It acts as a gonadotropin by
80 promoting vitellogenesis in females and accessory gland protein synthesis in males (Wilson et
81 al., 2003; Santos et al., 2019). Recent studies further implicate JH in the regulation of courtship
82 behavior, sleep, and aging (Wijesekera et al., 2016; Wu et al., 2018; Yamamoto et al., 2013).
83 In contrast to the well-characterized downstream effects of JH signaling, the regulation of JH
84 synthesis remains relatively understudied in *D. melanogaster*. Notably, several enzymes
85 catalyzing reactions in the late steps have yet to be fully identified (Fig. 1). For example, mutants
86 lacking *jhamt* do not exhibit the pupal lethal phenotype observed in *Met* and *gce* double mutants
87 (Abdou et al., 2011; Wen et al., 2015), suggesting the existence of other methyltransferase(s) that
88 compensate for the loss of Jhamt. Moreover, a canonical CYP epoxidase is not conserved in
89 higher dipterans. A recent study identified Cyp6g2 as an epoxidase in *D. melanogaster* (Jia et al.,
90 2024). This enzyme synthesizes not only JH III, the predominant form of JH in insects, but also
91 JH III bisepoxide (JHB3), a higher dipteran-specific JH (Richard et al., 1989). However, the

existence of additional epoxidases remains plausible, as *Cyp6g2* disruption does not cause severe developmental defects as compared to JH receptor knockouts (Abdou et al. 2011; Jia et al. 2024).

In the present study, we investigated CYP genes that are highly expressed in the CA in *D. melanogaster* and identified a second epoxidase, Cyp6a13. Combined knockouts of *jhamt*, *Cyp6g2*, and *Cyp6a13* caused severe developmental defects similar to those observed in *Met* and *gce* double mutants. These mutants also showed reduced egg production, a phenotype commonly associated with JH deficiency. Furthermore, we confirmed the enzymatic functions of these genes using a heterologous expression system and *ex vivo* tissue culture. Collectively, our results indicate that Cyp6g2 and Cyp6a13 function cooperatively to mediate JH biosynthesis in *D. melanogaster*.

2. Materials and methods

2.1. Flies

Flies were raised at 25°C under a 12 h-light and 12 h-dark photocycle on a standard cornmeal diet (Fujinaga et al., 2025). The control strain w^{1118} and transgenic flies were obtained from the Bloomington *Drosophila* Stock Center (BDSC), Vienna *Drosophila* Resource Center (VDRC), Tzumin Lee, Michael E. Adams, and Michael B. O'Connor, as listed in Table S1. Complementary DNA (cDNA) fragments of *jhamt*, *Cyp6g2*, and *Cyp6a13* were obtained from cDNA clones AT13581, IP03155, and LD25139, respectively, from the *Drosophila* Genomic Resource Center (DGRC) and cloned into the *pUAST* vector (Table S2) to generate UAS constructs. Transgenic flies were generated by BestGene Inc. Null mutant flies were generated by deleting most or all of the coding sequences of the target genes using the CRISPR-Cas9 system. Mutagenesis of *Met*, *gce*, and *Cyp6a13* was performed following the protocol developed by Kondo and Ueda (2013), with slight modifications as described in our previous study (Fujinaga et al., 2025). Briefly, two guide RNA (gRNA) target sequences for each genomic locus were inserted into *pBFv-U6.2* vectors using oligonucleotide pairs listed in Table S3, and a plasmid with two gRNA sequences was constructed for each gene. For the *Met* and *gce* mutant strains, embryonic injection of the plasmids and generation of G1 mutants were performed by BestGene Inc. For the *Cyp6a13* mutant strain, a transgenic strain carrying the plasmid at the *attP2* site was generated by BestGene Inc. The obtained *U6-gRNA* flies were crossed with *nos-Cas9* flies to induce mutagenesis in germ cells. Mutations were confirmed using primers designed outside the target sites (Table S3). Gene disruption mutants of *jhamt* and *Cyp6g2* were generated by WellGenetics Inc., using CRISPR-based homologous recombination to insert

125 fluorescent protein-coding sequences. All mutants were backcrossed with the w^{1118} control strain
126 for at least four generations to minimize off-target effects and standardize genetic backgrounds.
127
128 **2.2. Cell lines**
129 Human embryonic kidney (HEK) 293 cells were obtained from Michael E. Adams. Cells
130 were maintained in 75 cm^2 flasks (VWR) in a humidified incubator at 37°C and 5% CO_2 in
131 Dulbecco's Modified Eagle's Medium (DMEM) with 4.5 mg/mL glucose, L-glutamine, and
132 sodium pyruvate (Corning, #10-013-CV) containing 10% fetal bovine serum (Corning, #10082-
133 139) and 1% penicillin-streptomycin (Thermo Fisher Scientific, #15-140-122).
134
135 **2.3. Transcriptome analysis using public RNA sequencing data**
136 Public RNA sequencing data (GSE229077) were obtained from the Gene Expression
137 Omnibus (Roger et al., 2023). Reads were aligned to the *Drosophila* genome (BDGP6.46,
138 Ensembl) using Hisat2 (Kim et al., 2019). Aligned reads per gene were counted using SAMtools
139 (Danecek et al., 2021) and featureCount (Liao et al., 2014). Reads per kilobase per million
140 (RPKM) were calculated based on total reads and are listed in Table S4. Genes with expression
141 levels above 20 RPKM were considered to be highly expressed.
142
143 **2.4. Visualization of *jhamt-LexA* expression patterns**
144 Wandering larvae and three-day post-eclosion adult males expressing *jhamt-LexA*-driven
145 *LexAop-mCD8::GFP* were chilled on ice for 10 min. GFP expression patterns in the whole body
146 were observed using a SteREO Discovery.V12 microscope (Zeiss). Detailed expression patterns
147 of *jhamt-LexA* were visualized by immunostaining. Tissues were dissected in phosphate-buffered

148 saline (PBS) (Fisher Scientific, #BP399-1), fixed with 4% paraformaldehyde (PFA) (Electron
149 Microscopy Sciences, #157-8) in PBS containing 0.1% TritonX-100 (4% PFA/PBSTx) for 20
150 minutes at room temperature (RT), and washed multiple times with PBSTx. Tissues were
151 blocked with 5% normal goat serum (NGS) (Sigma-Aldrich, G9023) in PBSTx for at least one
152 hour at RT, incubated overnight at 4°C with chicken anti-GFP antibody (1:500, Abcam,
153 #ab13970) in PBSTx with 5% NGS, and then washed multiple times with PBSTx. They were
154 then incubated for two hours at RT with goat anti-chicken IgG conjugated to Alexa Fluor 488
155 (Life Technologies, #A-11039) in PBSTx with 5% NGS, followed by additional PBSTx washes.
156 DNA was stained with Hoechst 33342 (1:2,000, Life Technologies, #H3570) for 30 min at RT.
157 After washing, tissues were mounted in Vectashield H-1000 (Vector Laboratories, #H-1000-10)
158 and observed using a Zeiss Axio Imager M2 equipped with ApoTome.2 (Zeiss).
159

160 **2.5. Total RNA extraction and quantitative reverse transcription PCR**

161 Total RNA was extracted from tissues using TRIzol reagent (Thermo Fisher Scientific,
162 #15596018), and purified with the RNeasy Mini Kit (Qiagen, #74106) following the
163 manufacturers' instructions. cDNA was synthesized from purified RNA using PrimeScript RT
164 Master Mix (Takara Bio, #RR036A). Quantitative reverse transcription (qRT)-PCR was
165 performed on a CFX Connect Real-Time PCR Detection System (Bio-Rad) using AzuraView™
166 GreenFast qPCR Blue Mix LR (Azura Genomics, AZ-2320). Serial dilutions of plasmids
167 containing target sequences were used as standards for absolute quantification. Transcript levels
168 of mRNA were normalized to the internal control gene, *rp49*, as in Okamoto et al., 2018. Primers
169 are listed in Table S3.
170

171 **2.6. RNA probe synthesis**

172 Coding sequences of the target genes were PCR-amplified using T7- and SP6-tagged primers
173 listed in Table S3. Digoxigenin (DIG)-labelled RNA was synthesized using the DIG RNA
174 Labeling Kit (SP6/T7, Roche, #11175025910) following the manufacturer's protocol. Following
175 DNase treatment at 37°C for 15 min, labelled RNA was purified using the RNeasy Mini Kit.
176 RNA was hydrolyzed at 60°C for 45 min in alkaline solution (80 mM sodium bicarbonate, 120
177 mM sodium carbonate, and 10 mM DTT), and the reaction was terminated with neutralization
178 buffer (300 mM sodium acetate, 1% acetic acid, and 10 mM DTT). RNA probes were purified
179 by ethanol precipitation and stored at -20°C.

180

181 **2.7. Whole mount *in situ* hybridization**

182 Wandering larvae of w^{1118} were cut in half in PBS, and posterior segments were flipped to
183 expose internal organs. Tissues were fixed in 4% PFA in PBS for 20 min, then washed three
184 times with PBS containing 0.2% Tween 20 (PBST). Tissues were then rinsed three times with
185 methanol. After washing with 90% methanol containing 50 mM EGTA, half the volume was
186 replaced to 4% PFA three times, followed by fixation in 4% PFA in PBS for 20 min. Tissues
187 were treated with 50 µg/mL Proteinase K (Roche, #3115828001) in PBST for 5 min, followed by
188 fixation in 4% PFA in PBS for 20 min. After washing with PBST, tissues were incubated in the
189 pre-hybridization buffer (50% formamide, saline sodium citrate, 100 µg/mL heparin, 100 µg/mL
190 yeast RNA, 10 mM DTT, and 0.1% Tween 20) at 60°C for one hour. RNA probes (200 ng/mL
191 for *jhamt* and *Cyp6g2*, 1,000 ng/mL for *Cyp6a13*) were denatured in the hybridization solution
192 (10% dextran sulfate-containing pre-hybridization solution) at 80°C for 15 min, followed by
193 chilling on ice for 5 min. The RNA probe solution was then applied to tissues for overnight

194 incubation at 60°C. Tissues were washed six times for 30 min with the washing solution (50%
195 formamide, saline sodium citrate, and 0.1% Tween 20), then blocked with the blocking solution
196 (2% bovine serum albumin in PBST) for 30 min. Alkaline phosphatase-conjugated anti-DIG
197 antibody (Roche, #11093274910) diluted in the blocking solution (1:3,000) was applied
198 overnight at 4°C. Following three 20-min PBST washes, tissues were incubated in the alkaline
199 phosphatase buffer (100 mM Tris-hydrochloride, 100 mM sodium chloride, 50 mM magnesium
200 chloride, and 0.1% Tween 20, pH 9.5), followed by colorimetric development with nitro blue
201 tetrazolium (Roche, #11383213001) and 5-bromo-4-chloro-3-indolyl phosphate (Roche,
202 #11383221001) for one hour. After washing, tissues were permeated with glycerol, and the
203 central nervous system-ring gland (RG) complexes were dissected and imaged using a SteREO
204 Discovery.V12 microscope (Zeiss) and an Olympus BX53 microscope with a DP26 CCD
205 camera.
206
207 **2.8. Scoring of lethal stages**
208 Eggs of each genotype were collected on a grape juice plate with yeast powder. Larvae were
209 collected within two hours after hatching and reared on the standard cornmeal diet until 48 hours
210 after hatching. Homozygous mutants were selected based on the absence of the balancer
211 chromosome carrying GFP or RFP, followed by separation of males and females. Larvae were
212 then transferred to new vials (8-25 larvae/vial) containing the standard cornmeal diet with or
213 without specific concentrations of FA (Echeron Biosciences, #S-0151), MF (Echeron
214 Biosciences, #S-0153), JH III (Echeron Biosciences, #S-0155), or JHB3 (Echeron Biosciences,
215 #S-0157). Dead larvae and prepupae were counted six days after hatching, after which the size of
216 the pupal cases was measured. Animals that underwent head eversion were scored as pupae.

217 Dead pupae, early lethal adults, and normal adults were scored 10 days after hatching. The
218 developmental lethal phenotype was scored as follows: larval lethal = 0, prepupal lethal = 1,
219 pupal lethal = 2, early adult lethal = 3, and normal development = 4. The average score of each
220 genotype was calculated as the developmental score, and it was plotted along with the *Kruppel*
221 *homolog 1* (*Kr-h1*) expression level or the pupal case size for various genotypes using R. The
222 correlation coefficient and *p*-value (Pearson's test) for each plot were calculated using R.
223

224 **2.9. Fecundity assay**

225 Newly hatched larvae of selected genotypes were raised on the cornmeal diet until 48 hours
226 after hatching. Larvae were then transferred to vials at a density of fewer than 40 larvae per 3 g
227 of the diet and kept until eclosion. Five virgin females of each genotype were collected within
228 six hours after eclosion and kept in the vials containing the cornmeal diet with or without 0.5
229 ppm MF or JH III. Twenty-four hours later, three w^{1118} males were added for mating. After
230 another 24 hours, flies were transferred to vials containing agarose-solidified grape juice with
231 yeast powder. Flies were transferred into fresh vials every 24 hours, and the number of eggs in
232 each vial was counted under a stereomicroscope.
233

234 **2.10. Enzymatic conversion assay in HEK293 cells**

235 Coding sequences of *jhamt*, *Cyp6g2*, and *Cyp6a13* for heterologous expression in HEK293
236 cells were obtained from cDNA clones AT13581, IP03155, and LD25139, respectively, as listed
237 in Table S2, and cloned into the *pcDNA3.1(+)* vector. HEK293 cells at a density of 2 x 10^5 cells
238 in 2 mL of the culture medium were seeded on a 6-well clear flat bottom microplate (Bioland
239 Scientific, #703003). After preincubation for 24 hours, 0.3 µg of the *jhamt*-encoding plasmid and

240 0.9 μg of CYP enzyme-encoding plasmids were transfected using Attractene transfection reagent
241 (Qiagen, #301005) according to the manufacture's instruction. The empty vector was transfected
242 for control experiments. After 48 hours of incubation, 5×10^5 cells were transferred into glass
243 vials (Agilent, #5183-2068) containing S-adenosyl methionine (Millipore, #A7007; final
244 concentration: 50 μM) and the esterase inhibitor Paraoxon (Fisher Scientific, #NC0811417; final
245 concentration: 1 μM) in 720 μL of the FBS-free medium. Three hours after incubation, 7.2 μL of
246 1 mM FA was added, and the cells were further incubated for 18 hours. After mixing with 80 μL
247 of acetonitrile, vials were stored at -20°C until extraction.
248
249 **2.11. *Ex vivo* Ring gland culture**
250 Ten RGs of selected genotypes were dissected from wandering larvae and preincubated in
251 720 μL of Schneider's *Drosophila* medium (Gibco, #21-720-024) in a glass vial for 30 min.
252 After adding 7.2 μL of 1 mM FA to the culture medium, the RGs were incubated for four hours
253 at 25°C. After incubation, 80 μL of acetonitrile was added, and the samples were stored at -20°C
254 until extraction.
255
256 **2.12. Hemolymph collection**
257 Wandering third instar larvae were rinsed in PBS and dried on tissue paper. The cuticle was
258 carefully torn to release the hemolymph onto a parafilm membrane. Ten μL of the hemolymph
259 was collected and mixed with extraction solution (90 μl of 0.9% sodium chloride solution and 10
260 μL of acetonitrile) in a glass insert vial (Agilent, #5181-1270).
261
262 **2.13. Sesquiterpenoid extraction**

263 Extraction of sesquiterpenoids was performed based on the previous study (Sarro et al., 2021,
264 adapted from Kai et al., 2018) with modifications. For hemolymph samples, 2 ng of citronellol
265 (Millipore, #W230915) or 4 ng of deuterium-labelled JH III (JH III-d3) (LGC Ltd., #E589402)
266 was added as an internal standard for gas chromatography-mass spectrometry (GC-MS) analysis
267 or liquid chromatography-mass spectrometry (LC-MS) analysis, respectively. After 100 µL of
268 hexane was added, the samples were vigorously mixed for 30 seconds. The samples were then
269 allowed to sit for 5 min, followed by centrifugation at 1,000 x g for 5 min. The hexane layer was
270 transferred to a new glass vial using a Hamilton syringe (Hamilton, #80600), and the extraction
271 was repeated. For LC-MS analysis, the pooled hexane extract was concentrated by CentriVap
272 concentrator (Labconco) to 100 µL. After adding 100 µL of methanol, the remaining hexane was
273 evaporated. For extraction from the culture medium, 16 ng of citronellol or 4 ng of JH III-d3 was
274 added. After adding 800 µL of hexane, the samples were vigorously mixed for 30 seconds. The
275 hexane layer was then collected as described above.
276
277 **2.14. Sesquiterpenoid determination**
278 For developing the simultaneous extraction method, FA, MF, JH III, and JHB3 (100 ng each)
279 were added to the extraction solution (400 or 720 µl of 0.9% sodium chloride solution and 400 or
280 80 µl of acetonitrile) in the glass vial. Compounds were extracted as described above, and the
281 hexane extract was concentrated to 100 µl using CentriVap concentrator (Labconco). After
282 adding 100 µl of methanol, the remaining hexane was evaporated. Extracted sesquiterpenoids
283 were analyzed using a 1220 Infinity LC system (Agilent Technologies) with a Vydac 218TP C18
284 HPLC column (100 mm x 4.6 mm, 5 µm particle size, Grace). HPLC-grade acetonitrile and
285 water were used as the liquid phase in a binary gradient flow (Pump A: 20% acetonitrile/80%

286 water, Pump B: 100% acetonitrile). Ten µl of the extracted sample or authentic standards was
287 injected, and absorbance at 217 nm was recorded for peak area analyses.
288 For biological samples, MF and JH III were detected and quantified using a Thermo
289 Scientific Trace 1310 GC-MS equipped with an AI 1310 autosampler and a TSQ Duo triple
290 quadrupole mass spectrometer (Thermo Scientific), following the method described previously
291 (Sarro et al., 2021) with slight modifications. Detailed parameters for selected reaction
292 monitoring were listed in Table S5. Authentic standards of MF and JH III were used to generate
293 standard curves. Peak areas of the target compounds were normalized by the peak area of
294 citronellol (10 ng/mL). JHB3 levels were determined using LC-MS at the UC Riverside
295 Metabolomics Core based on the previous study (Ramirez et al., 2020) with modifications.
296 Liquid chromatography separation was performed by an ultra-performance liquid
297 chromatography system (ACQUITY UPLC I-Class PLUS, Waters) equipped with an ACQUITY
298 UPLC BEH C18 column (2.1 × 100 mm, 1.7 µm, Waters). The column temperature was
299 maintained at 35°C. Gradient separation was performed between 0.1% formic acid in water
300 (mobile phase A) and 0.1% formic acid in acetonitrile (mobile phase B) at a flow rate of 0.3
301 mL/min. The gradient program was as follows: 4% B at 0 min; increase to 10% B in 2 min;
302 increase to 80% B in 12 min and hold for 0.1 min; increase again to 100% B in 0.9 min and hold
303 for another 0.1 min; then return to 4% B in 1.4 min; for a total run time of 16.5 min. Detection
304 was performed using a Xevo TQ-XS mass spectrometry system (Waters) equipped with an
305 electrospray ionization interface. The instrument was operated in multiple reaction monitoring
306 mode as described in Table S6. Authentic standards of FA, JH III, and JHB3 were used to
307 generate standard curves. Peak areas were normalized to the peak area of JH III-d3 (40 ng/mL).
308

309 **2.15. Phylogenetic analysis**

310 The unrooted maximum-likelihood phylogenetic tree was generated using MEGAX (Kumar
311 et al., 2018). Amino acid sequences of CYP 3 clan in *D. melanogaster* were selected using
312 Flybase (Öztürk-Çolak et al., 2024). Entire amino acid sequences of the enzymes in the housefly
313 (*Musca domestica*), yellow fever mosquito (*Aedes aegypti*), silkmoth (*Bombyx mori*), western
314 honey bee (*Apis mellifera*), red flour beetle (*Tribolium castaneum*), pea aphid (*Acyrthosiphon*
315 *pisum*), and Nevada termite (*Zootermopsis nevadensis*) were obtained from the National Center
316 for Biotechnology Information database (Sayers et al., 2022) using full length amino acid
317 sequences of *D. melanogaster* proteins as queries. The protein names and GenBank accession
318 numbers are listed in Table S7.

319

320

321 **3. Results**

322 **3.1. Identification of CYPs highly expressed in the CA during early metamorphosis**

323 We first investigated CYP enzymes that are highly expressed in the CA. In *D. melanogaster*,
324 the CA is located within the RG, a composite endocrine organ (Zhang et al., 2022). We therefore
325 analyzed previously published RNA sequencing data of the RGs from larvae at the wandering
326 stage (Roger et al., 2023), when JH titers are known to be high (Sliter et al., 1987). We identified
327 12 CYP genes highly expressed in the RG (Table S4), including four ecdysteroid biosynthetic
328 enzymes that are highly expressed in the prothoracic gland (Niwa and Niwa, 2025), which also
329 constitutes the RG.

330 We next compared the expression levels of these CYP genes in the RG using qRT-PCR
331 between control and CAX larvae. As the *Gal4* drivers previously used to induce CAX are also
332 expressed in the salivary glands (Liu et al., 2009; Riddiford et al., 2010), we used a more CA-
333 specific driver, *jhamt-LexA* (Ohhara et al., 2018; Fig. S1A), to ablate the CA by expressing pro-
334 apoptotic genes (Ren et al., 2018; Fig. S1B). Among these genes, *Cyp6g2* and *Cyp6a13* showed
335 high expression in the RG of control larvae as compared to CAX larvae (Fig. 2A), indicating that
336 these genes are highly expressed in the CA, similar to *jhamt*. Absolute quantification of the gene
337 expression revealed that *Cyp6g2* is expressed at a level more than 20 times higher than that of
338 *Cyp6a13* in the control RG (Fig. S2). *In situ* hybridization further confirmed the expression of
339 these genes in the CA, although the signal of the *Cyp6a13* antisense probe was weaker than that
340 of *jhamt* or *Cyp6g2* due to its lower expression in the CA (Fig. 2B).

341

342 **3.2. Combined mutations of the enzymes cause metamorphic defects similar to JH receptor**
343 **mutants**

344 We next generated null mutant alleles (Fig. S3) and analyzed the mutant flies to investigate
345 contributions of these enzymes to *Drosophila* development. We also used our newly generated
346 *Met*, *gce* double mutant line (Met^{45B}, gce^{2Cl}) as a JH signaling-deficient control throughout this
347 study, in order to exclude the potential effects of the intact coding sequence of the Met^{27} allele
348 (Wilson and Ashok, 1998) used in the previously reported *Met*, *gce* double mutant (Abdou et al.,
349 2011).
350 Consistent with previous studies on JH signaling-deficient flies (Liu et al., 2009; Riddiford et
351 al., 2010; Abdou et al., 2011), our new CAX flies died at different stages of metamorphosis (Fig.
352 3A). Based on this, we observed and classified developmental lethality of the mutant flies into
353 the following five categories: larval lethal, prepupal lethal (PPL; characterized by incomplete air
354 bubble translocation and/or head eversion), pupal lethal (PL), early adult lethal (EAL; defined as
355 death within 24 hours after eclosion without wing expansion), and normal development. While
356 almost all control flies (w^{1118}) developed normally (Fig. 3B), most *Met*, *gce* double mutant flies
357 died during pupation, with some showing the pupal lethality. Many CAX flies reached the pupal
358 stage but eventually died during adult development or shortly after eclosion. *jhamt* single mutant
359 flies showed mild phenotypes, as previously reported (Wen et al., 2015; Jia et al., 2024); most of
360 these flies became adults, although about half of them died shortly after eclosion. Single mutants
361 of *Cyp6g2* or *Cyp6a13* did not exhibit significant developmental defects, whereas combining
362 them with the *jhamt* mutation showed much more severe phenotype, similar to *Met*, *gce* double
363 mutants. Most *jhamt*, *Cyp6g2* double mutant flies died during or after pupation. *jhamt*, *Cyp6a13*
364 double mutants showed slightly milder phenotypes than *jhamt*, *Cyp6g2* double mutants, although
365 they were still significantly more severe than *jhamt* single mutant flies. *Cyp6g2*, *Cyp6a13* double
366 mutants also showed mild lethal phenotypes. *jhamt*, *Cyp6g2*, *Cyp6a13* triple mutants showed

367 severe phenotypes similar to *jhamt*, *Cyp6g2* double mutants. Altogether, these findings suggest
368 that Jhamt, Cyp6g2, and Cyp6a13 function as JH synthetic enzymes and may have overlapping
369 functions, as single mutants exhibited only mild phenotypes. Moreover, tissue specific
370 knockdown using a *Gal4* driver expressed in the CA also suggested the JH synthetic activity of
371 these enzymes in the CA (Fig. 3C). Single knockdowns of the CYPs did not cause significant
372 developmental lethality. However, combined knockdown of *jhamt* and *Cyp6g2* or *jhamt* and
373 *Cyp6a13* induced severe developmental defects, similar to the corresponding mutant
374 combinations. Furthermore, the severity of developmental phenotypes of CAX and the mutant
375 flies correlated with expression levels of a JH response gene, *Kr-h1* (Fig. 3D). Flies with mild
376 developmental phenotypes (CAX; $jhamt^{-}$; and $Cyp6g2^{-}$, $Cyp6a13^{-}$) exhibited moderate reduction
377 of *Kr-h1* expression compared to w^{1118} control, while those with more severe phenotypes
378 (Met^{45B}, gce^{2C1}; $jhamt^{-}$, $Cyp6g2^{-}$; $jhamt^{-}$, $Cyp6a13^{-}$; and $jhamt^{-}$, $Cyp6g2^{-}$, $Cyp6a13^{-}$) showed
379 further reduction of *Kr-h1* expression levels. This strong correlation was confirmed by the
380 correlation analysis (Fig. 3E), further suggesting the involvement of these enzymes in JH
381 biosynthesis.

382 We also analyzed the pupal body size of CAX and the mutant flies (Fig. S4A). Previous
383 studies have shown that JH-deficient flies exhibit a smaller body size along with slight
384 developmental delay (Riddiford et al., 2010; Mirth et al., 2014). Consistent with this, *Met*, *gce*
385 double mutant, CAX, *jhamt*, *Cyp6g2* double mutant, and *jhamt*, *Cyp6g2*, *Cyp6a13* triple mutant
386 flies were significantly smaller than w^{1118} control flies in both sexes. Indeed, correlation analyses
387 confirmed a strong correlation between developmental lethality and pupal body size reduction
388 (Fig. S4B and C). In contrast, pupariation timing was not significantly altered, although mutants
389 with high lethality tended to exhibit slightly delayed pupariation timing (Fig. S4D).

390

391 **3.3. Sesquiterpenoid feeding rescues developmental defects of the enzyme mutants**

392 In order to confirm that developmental defects of CAX flies and the mutants were caused by
393 impaired JH biosynthesis, we applied JHs and their precursors to the third instar larvae (Fig. 4A-
394 H). Control flies showed no developmental defects when treated with the sesquiterpenoids (Fig.
395 4A). As expected, no rescue was observed in *Met*, *gce* double mutants (Fig. 4B), as they lack the
396 molecular machinery to respond to JH. In contrast, developmental defects of CAX flies were
397 rescued by all terpenoids tested, particularly MF, JH III, and JHB3 (Fig. 4C). These control
398 experiments demonstrate that exogenous sesquiterpenoid application can successfully
399 compensate for endogenous JH functions without any harmful side effects during development.
400 It should be noted that MF, like JH III and JHB3, can also activate JH receptors, although its
401 activity is weaker than JH III and JHB3 (Jindra et al., 2015). The enzyme mutants were also
402 rescued by MF, JH III, and JHB3 in a dose-dependent manner (Fig. 4D-H), suggesting that the
403 lethality observed in the mutant flies was indeed due to reduced JH production. Conversely,
404 application of the JH precursor, FA, hardly rescued the enzyme mutants, suggesting that these
405 enzymes function downstream of FA in the JH biosynthetic pathway (Fig. 1). Interestingly,
406 significant rescue of the developmental lethality in CAX flies was observed when the higher
407 concentration (5 ppm) of FA was applied, potentially suggesting the existence of an alternative
408 JH biosynthetic machinery outside the CA.

409 We also performed rescue experiments of *jhamt*, *Cyp6g2* and *jhamt*, *Cyp6a13* double
410 mutants by overexpressing each enzyme in the CA (Fig. 4I and J). Consistent with their
411 functions in the CA, overexpression of the enzymes in their corresponding mutants significantly
412 rescued the developmental defects. Importantly, *Cyp6g2* overexpression significantly rescued

413 *jhamt*, *Cyp6a13* double mutants, whereas *Cyp6a13* overexpression did not rescue *jhamt*, *Cyp6g2*
414 double mutants. These results suggest that Cyp6g2 and Cyp6a13 may have overlapping roles in
415 JH biosynthesis in the CA, but Cyp6g2 likely has broader functions than Cyp6a13.
416
417 **3.4. Contribution of the enzymes to reproduction**
418 During metamorphosis, the CA and corpora cardiaca (CC) complex migrates toward the
419 ventral ganglion and eventually settles on the esophagus in *D. melanogaster* (Dai and Gilbert
420 1991; Fig. S1A). Although *Cyp6a13* expression levels were significantly lower than the other
421 enzymes (~1.5% compared to *jhamt* expression), transcripts of all the three enzyme-encoding
422 genes were detectable in the adult CA/CC complex (Fig. 5A-C). Among the three enzyme-
423 encoding genes, *jhamt* expression increased within 24 hours after eclosion, potentially reflecting
424 the elevated JH III titer after eclosion (Reiff et al., 2015; Sugime et al., 2017).
425 Given the functions of JHs as gonadotropic factors in adults (Santos et al., 2019), we next
426 measured the number of eggs laid by the mutant flies to assess the contributions of these
427 enzymes to reproduction (Fig. 5D). *jhamt* single mutant and *Cyp6g2*, *Cyp6a13* double mutant
428 females laid significantly fewer eggs compared to w^{1118} control (Fig. 5E). On the other hand,
429 neither *Cyp6g2* nor *Cyp6a13* single mutants displayed statistically significant reduction of the
430 number of laid eggs. These results suggest that Cyp6g2 and Cyp6a13 may compensate for each
431 other in JH production in adult females. Treatment with MF or JH III after eclosion significantly
432 increased the fecundity of females of all genotypes, further suggesting the importance of JH
433 signaling in reproduction in female flies.
434
435 **3.5. Cyp6g2 and Cyp6a13 are responsible for epoxidation of JH precursors**

436 To further investigate enzymatic activities *in vitro*, we modified the sesquiterpenoid
437 extraction described in Sarro et al. (2021) to enable simultaneous extraction of MF, JH III, and
438 JHB3 for GC-MS and LC-MS analyses. The modified hexane extraction method recovered
439 nearly 100% of FA, MF, JH III, and JHB3 (Fig. S5). Using this method, we conducted an
440 enzymatic conversion assay in HEK293 cells (Fig. 6A). Overexpression of *jhamt* induced
441 methylation of FA as expected from previous studies (Niwa et al., 2008), while its co-expression
442 with either *Cyp6g2* or *Cyp6a13* did not enhance MF production (Fig. 6B). In contrast, co-
443 expression of *Cyp6g2* with *jhamt* enhanced conversion of FA into JH III beyond the basal level
444 of JH III production observed in *jhamt* single overexpression (Fig. 6C), consistent with the
445 reported epoxidase activity of Cyp6g2 (Jia et al., 2024). Importantly, co-expression of *Cyp6a13*
446 with *jhamt* also promoted conversion of FA into JH III (Fig. 6C), suggesting that it encodes an
447 epoxidase similar to Cyp6g2.
448 Contrary to our expectations, JHB3 was not detected under any condition in the enzymatic
449 conversion assay in HEK293 cells. We speculate that an unknown cofactor present in the CA
450 may be necessary for JHB3 biosynthesis *in vivo*. We therefore conducted *ex vivo* culture of the
451 larval RGs to assess enzymatic activity of CYPs in the CA (Fig. 6D). JH III and JHB3 were
452 detected in the RGs from control larvae cultured with FA (Fig. 6E and F), confirming the
453 methylation and epoxidation activities in the cultured RGs. In the *Cyp6g2* mutant RG, JH III
454 production was significantly decreased (Fig. 6E), and JHB3 production was below the detection
455 limit (Fig. 6F). These results indicate that Cyp6g2 acts as an epoxidase that can produce both JH
456 III and JHB3. Although the RGs from the *Cyp6a13* single mutant larvae did not show
457 statistically significant reduction of JH III or JHB3 production, JH III was not produced in the

458 cultured RGs from the *Cyp6g2*, *Cyp6a13* double mutant larvae (Fig. 6E). This further suggests
459 that Cyp6a13 epoxidizes JH precursors to synthesize JH III.
460 Lastly, hemolymph JH levels were analyzed to confirm the JH biosynthetic activities of the
461 enzymes *in vivo*. In the hemolymph of wandering larvae, we could only detect JHB3, as the
462 reported amounts of larval JH III are far below our detection limit (~5 pg/μL hemolymph; Jones
463 et al., 2013; Wen et al., 2015; Barton et al., 2024). Compared to control, the hemolymph level of
464 JHB3 was significantly reduced in the *Cyp6a13* single mutant larvae, and it was not detected in
465 CAX larvae and the other mutants tested (Fig. 6G). Overall, our results demonstrate that both
466 Cyp6g2 and Cyp6a13 function as epoxidases in the CA to produce JHs *in vivo*.
467

468 **4. Discussion**

469 In the present study, we demonstrated that two CYP enzymes, Cyp6g2 and Cyp6a13,
470 function as epoxidases for JH biosynthesis in the *Drosophila* CA. Higher dipteran insects, known
471 as *Cyclorrhapha*, have lost the canonical sesquiterpenoid epoxidase CYP15 in their genomes
472 (Dermauw et al., 2020; Smykal and Dolezel, 2023). Instead, they possess CYP6 enzymes as
473 epoxidases: for example, Cyp6a1 has been identified as an MF epoxidase in the housefly *Musca*
474 *domestica* (Andersen et al., 1997). A recent study showed that Cyp6g2 is a major epoxidase for
475 JH production in *D. melanogaster* (Jia et al., 2024). The present study now adds *Drosophila*
476 Cyp6a13 to the list of CYP6 epoxidases. Considering that the RGs isolated from wandering
477 *Cyp6g2*, *Cyp6a13* double mutant larvae did not produce detectable levels of JHs (Fig. 6E and F),
478 it is likely that Cyp6g2 and Cyp6a13 are the only epoxidases that contribute to JH production in
479 the *Drosophila* CA, at least during the wandering stage. The relatively mild developmental
480 defects seen in *Cyp6g2*, *Cyp6a13* double mutants are likely due to the weak but significant JH
481 receptor-activating capacity of MF (Jindra et al., 2015; Wen et al., 2015).

482 JHB3 is a unique JH species in higher dipteran insects that have lost CYP15 epoxidases
483 (Smykal and Dolezel, 2023). It is therefore likely that JHB3 is a specific product of CYP6
484 epoxidases. Given that the *Cyp6g2* mutant RGs do not synthesize detectable amounts of JHB3 *ex*
485 *vivo*, Cyp6g2 may be the only epoxidase that can synthesize JHB3 in *D. melanogaster*. Although
486 the hemolymph level of JHB3 was drastically reduced in *Cyp6a13* single mutant larvae, this may
487 be due to the reduced production of JH III, the precursor of JHB3. The inferred functions of
488 CYP6 enzymes are summarized in Fig. 6H.

489 In *D. melanogaster*, it is known that the hemolymph JHB3 titer is much higher than that of
490 JH III (Wen et al., 2015; Ramirez et al., 2020). This is consistent with our hemolymph JH

491 analysis, in which we only detected JHB3. It is therefore interesting that comparable amounts of
492 JH III and JHB3 were produced in the RGs cultured *ex vivo*. A potential explanation for this is
493 that JH-degrading enzymes such as JH esterases and JH epoxide hydrolases (Kamita and
494 Hammock, 2010) may preferentially degrade JH III over JHB3. Although a previous *in vitro*
495 study showed that *Drosophila* JH esterase has similar affinity for both JH III and JHB3
496 (Campbell et al., 1998), another study suggested that high concentrations of JH esterase
497 preferentially degrades JH III when bound to its binding proteins (Touhara et al., 1995). Since
498 JHB3 does not bind to lipophorin, a major JH-binding protein (Trowell et al., 1994), JH esterase
499 may be less effective at degrading JHB3 as compared to JH III. Alternatively, there may be an *in*
500 *vivo* mechanism that enhances JHB3 production and release in the CA, which does not work in
501 our *ex vivo* culture. Elucidating molecular mechanisms behind the high titer of JHB3 in the
502 *Drosophila* hemolymph may help us better understand the physiological significance of this
503 higher dipteran-specific JH species.
504 *D. melanogaster* Cyp6g2 and Cyp6a13, as well as *M. domestica* Cyp6a1, are scattered within
505 the insect CYP3 clan, suggesting that their JH biosynthetic functions evolved independently (Fig.
506 S6). Enzymes in the CYP3 clan (such as Cyp6 and Cyp9 enzymes) are highly divergent in
507 insects, and many are known to have xenobiotic-detoxifying activities (Nauen et al., 2022).
508 *Drosophila* Cyp6g2 and *Musca* Cyp6a1 are also known for their detoxification roles (Feyereisen,
509 1999; Giang et al., 2025). Many other CYP3 clan enzymes catalyze epoxidation of their target
510 compounds as well (Feyereisen, 1999). It is therefore possible that other enzymes in this clan are
511 also capable of epoxidizing sesquiterpenoids, but only those expressed in the CA have obtained
512 JH biosynthetic functions. We could not find any other CYP enzymes specifically expressed in
513 the CA, suggesting that other *Drosophila* enzymes do not contribute to JH biosynthesis *in vivo*,

514 at least during the wandering stage. In contrast, it remains possible that other CYPs function as
515 JH synthases in peripheral tissues, as some studies suggest that JH biosynthesis occurs in other
516 organs, such as the adult gut (Rahman et al., 2017; Shianiou et al., 2023). These studies showed
517 that *jhamt* expression in the gut is responsible for maintaining cellular growth. Notably, *Cyp6a13*
518 is expressed not only in the CA, but also in peripheral tissues, according to Flybase expression
519 data (Öztürk-Çolak et al., 2024). It is therefore possible that Cyp6a13 acts with Jhamt for JH
520 biosynthesis in peripheral tissues.
521 In summary, our current work revealed that two CYP6 enzymes, Cyp6g2 and Cyp6a13,
522 function cooperatively to synthesize JH in the *Drosophila* CA. Further investigations of their
523 differential functions, along with identification of additional JH biosynthetic enzymes, are
524 expected to help us better understand both species-specific and conserved features of JH
525 signaling in insects.
526

527 **Conflict of interest**

528 The authors declare no competing interest.

529

530 **Acknowledgement**

531 We thank Vienna *Drosophila* Resource Center, Bloomington *Drosophila* Stock Center
532 (supported by NIH P40 OD018537), National Institute of Genetics, T. Lee, M. E. Adams, and M.
533 B. O'Connor for fly stocks; FlyBase for providing curated *Drosophila* genome information;
534 Metabolomics core at the University of California, Riverside for JHB3 determination;
535 *Drosophila* Genomics Resource Center (supported by NIH 2P40 OD010949) and National
536 Institute of Genetics for vectors and cDNA clones. This study was supported by the Japan
537 Society for the Promotion of Science (JSPS) KAKENHI 21H02521 to Y.O., a Postdoctoral
538 Fellowship for Research Abroad from JSPS to N.O., the Naito Foundation Subsidy for Dispatch
539 of Young Researchers Abroad to N.O., an NIH grant R01 AI171032 from NIAID to N.Y., and an
540 NIH grant R35 GM153331 from NIGMS to N.Y.

541

542 **Author contributions**

543 DF: conceptualization, methodology, investigation, formal analysis, writing – original draft,
544 writing – review and editing. YO: methodology, investigation, funding acquisition, writing –
545 review and editing. NO: investigation, funding acquisition, writing – review and editing. HC:
546 generation of *Met*, *gce* mutant flies, writing – review and editing. KM: methodology for
547 sesquiterpenoid determination, writing – review and editing. NY: conceptualization, funding
548 acquisition, project administration, supervision, writing – review and editing.

549

550 **Reference**

551 Abdou, M.A., He, Q., Wen, D., Zyaan, O., Wang, J., Xu, J., Baumann, A.A., Joseph, J., Wilson,
552 T.G., Li, S., Wang, J., 2011. *Drosophila* Met and Gce are partially redundant in transducing
553 juvenile hormone action. *Insect Biochem. Mol. Biol.* 41, 938–945.
554 https://doi.org/10.1016/j.ibmb.2011.09.003

555 Andersen, J.F., Walding, J.K., Evans, P.H., Bowers, W.S., Feyereisen, R., 1997. Substrate
556 specificity for the epoxidation of terpenoids and active site topology of house fly cytochrome
557 P450 6A1. *Chem. Res. Toxicol.* 10, 156–164. https://doi.org/10.1021/tx9601162

558 Barton, L.J., Sanny, J., Packard Dawson, E., Nouzova, M., Noriega, F.G., Stadtfeld, M.,
559 Lehmann, R., 2024. Juvenile hormones direct primordial germ cell migration to the embryonic
560 gonad. *Curr. Biol.* 34, 505–518.e6. https://doi.org/10.1016/j.cub.2023.12.033

561 Bellés, X., Martín, D., Piulachs, M.D., 2005. The mevalonate pathway and the synthesis of
562 juvenile hormone in insects. *Annu. Rev. Entomol.* 50, 181–199.
563 https://doi.org/10.1146/annurev.ento.50.071803.130356

564 Campbell, P.M., Oakeshott, J.G., Healy, M.J., 1998. Purification and kinetic characterisation of
565 juvenile hormone esterase from *Drosophila melanogaster*. *Insect Biochem. Mol. Biol.* 28, 501–
566 515. https://doi.org/10.1016/S0965-1748(98)00037-X

567 Daimon, T., Kozaki, T., Niwa, R., Kobayashi, I., Furuta, K., Namiki, T., Uchino, K., Banno, Y.,
568 Katsuma, S., Tamura, T., Mita, K., Sezutsu, H., Nakayama, M., Itoyama, K., Shimada, T.,
569 Shinoda, T., 2012. Precocious metamorphosis in the juvenile hormone-deficient mutant of the

570 silkworm, *Bombyx mori. PLoS Genet.* 8, e1002486.
571 https://doi.org/10.1371/journal.pgen.1002486

572 Dai, J.D., Gilbert, L.I., 1991. Metamorphosis of the corpus allatum and degeneration of the
573 prothoracic glands during the larval-pupal-adult transformation of *Drosophila melanogaster*: a
574 cytophysiological analysis of the ring gland. *Dev. Biol.* 144, 309–326.
575 https://doi.org/10.1016/0012-1606(91)90424-2

576 Danecek, P., Bonfield, J.K., Liddle, J., Marshall, J., Ohan, V., Pollard, M.O., Whitwham, A.,
577 Keane, T., McCarthy, S.A., Davies, R.M., Li, H., 2021. Twelve years of SAMtools and
578 BCFtools. *Gigascience.* 10, giab008. https://doi.org/10.1093/gigascience/giab008

579 Defelipe, L.A., Dolghih, E., Roitberg, A.E., Nouzova, M., Mayoral, J.G., Noriega, F.G.,
580 Turjanski, A.G., 2011. Juvenile hormone synthesis: "esterify then epoxidize" or "epoxidize then
581 esterify"? Insights from the structural characterization of juvenile hormone acid
582 methyltransferase. *Insect Biochem. Mol. Biol.* 41, 228–235.
583 https://doi.org/10.1016/j.ibmb.2010.12.008

584 Dermauw, W., Van Leeuwen, T., Feyereisen, R., 2020. Diversity and evolution of the P450
585 family in arthropods. *Insect Biochem. Mol. Biol.* 127, 103490.
586 https://doi.org/10.1016/j.ibmb.2020.103490

587 Feyereisen, R., 1999. Insect P450 enzymes. *Annu. Rev. Entomol.* 44, 507–533.
588 https://doi.org/10.1146/annurev.ento.44.1.507

589 Fujinaga, D., Nolan, C., Yamanaka, N., 2025. Functional characterization of eicosanoid
590 signaling in *Drosophila* development. *PLoS Genet.* 21, e1011705.
591 https://doi.org/10.1371/journal.pgen.1011705

592 Giang, A., Martelli, F., Fusetto, R., Nero, T.L., Lueke, B., Nauen, R., Batterham, P., 2025.
593 Functional and structural insights into P450-mediated resistance: The role of Cyp6g1 and
594 Cyp6g2 in the metabolism of neonicotinoids in *Drosophila melanogaster*. *Pestic. Biochem.*
595 *Physiol.* 212, 106451. https://doi.org/10.1016/j.pestbp.2025.106451

596 Jia, Q., Yang, L., Wen, J., Liu, S., Wen, D., Luo, W., Wang, W., Palli, S.R., Sheng, L., 2024.
597 Cyp6g2 is the major P450 epoxidase responsible for juvenile hormone biosynthesis in
598 *Drosophila melanogaster*. *BMC Biol.* 22, 111. https://doi.org/10.1186/s12915-024-01910-4

599 Jindra, M., Palli, S.R., Riddiford, L.M., 2013. The juvenile hormone signaling pathway in insect
600 development. *Annu. Rev. Entomol.* 58, 181–204. https://doi.org/10.1146/annurev-ento-120811-
601 153700

602 Jindra, M., Uhlirova, M., Charles, J.P., Smykal, V., Hill, R.J., 2015. Genetic evidence for
603 function of the bHLH-PAS protein Gce/Met as a juvenile hormone receptor. *PLoS Genet.* 11,
604 e1005394. https://doi.org/10.1371/journal.pgen.1005394

605 Jindra, M., 2019. Where did the pupa come from? The timing of juvenile hormone signalling
606 supports homology between stages of hemimetabolous and holometabolous insects. *Philos.*
607 *Trans. R. Soc. Lond. B Biol. Sci.* 374, 20190064. https://doi.org/10.1098/rstb.2019.0064

608 Jindra, M., Noriega, F.G., 2025. Juvenile hormone signaling. In: Yamanaka N., Atkinson, P.W.
609 (Eds.), Comprehensive Molecular Insect Science (2nd edition). Elsevier Inc.

610 Jones, G., Teal, P., Henrich, V.C., Krzywonos, A., Sapa, A., Wozniak, M., Smolka, J., Jones, D.,
611 2013. Ligand binding pocket function of *Drosophila* USP is necessary for metamorphosis. *Gen.*
612 *Comp. Endocrinol.* 182, 73–82. https://doi.org/10.1016/j.ygcen.2012.11.009

613 Kai, Z.P., Yin, Y., Zhang, Z.R., Huang, J., Tobe, S.S., Chen, S.S., 2018. A rapid quantitative
614 assay for juvenile hormones and intermediates in the biosynthetic pathway using gas
615 chromatography tandem mass spectrometry. *J. Chromatogr. A.* 1538, 67–74.
616 https://doi.org/10.1016/j.chroma.2018.01.030

617 Kamita, S.G., Hammock, B.D., 2010. Juvenile hormone esterase: biochemistry and structure. *J.*
618 *Pestic. Sci.* 35, 265–274. https://doi.org/10.1584/jpestics.R10-09

619 Kayukawa, T., Minakuchi, C., Namiki, T., Togawa, T., Yoshiyama, M., Kamimura, M., Mita,
620 K., Imanishi, S., Kiuchi, M., Ishikawa, Y., Shinoda, T., 2012. Transcriptional regulation of
621 juvenile hormone-mediated induction of Krüppel homolog 1, a repressor of insect
622 metamorphosis. *Proc. Natl. Acad. Sci. U.S.A.* 109, 11729–11734.
623 https://doi.org/10.1073/pnas.1204951109

624 Kim, D., Paggi, J.M., Park, C., Bennett, C., Salzberg, S.L., 2019. Graph-based genome
625 alignment and genotyping with HISAT2 and HISAT-genotype. *Nat. Biotechnol.* 37, 907–915.
626 https://doi.org/10.1038/s41587-019-0201-4

627 Kondo, S., Ueda, R., 2013. Highly improved gene targeting by germline-specific Cas9
628 expression in *Drosophila*. *Genetics.* 195, 715–721. https://doi.org/10.1534/genetics.113.156737

629 Konopova, B., Jindra, M., 2007. Juvenile hormone resistance gene Methoprene-tolerant controls
630 entry into metamorphosis in the beetle *Tribolium castaneum*. *Proc. Natl. Acad. Sci. U.S.A.* 104,
631 10488–10493. https://doi.org/10.1073/pnas.0703719104

632 Konopova, B., Smykal, V., Jindra, M., 2011. Common and distinct roles of juvenile hormone
633 signaling genes in metamorphosis of holometabolous and hemimetabolous insects. *PLoS ONE* 6,
634 e28728. https://doi.org/10.1371/journal.pone.0028728

635 Kumar, S., Stecher, G., Li, M., Knyaz, C., Tamura, K., 2018. MEGA X: Molecular evolutionary
636 genetics analysis across computing platforms. *Mo.l Biol. Evol.* 35, 1547–1549.
637 https://doi.org/10.1093/molbev/msy096

638 Liao, Y., Smyth, G.K., Shi, W., 2014. featureCounts: an efficient general purpose program for
639 assigning sequence reads to genomic features. *Bioinformatics.* 30, 923–930.
640 https://doi.org/10.1093/bioinformatics/btt656

641 Liu, Y., Sheng, Z., Liu, H., Wen, D., He, Q., Wang, S., Shao, W., Jiang, R.J., An, S., Sun, Y.,
642 Bendena, W.G., Wang, J., Gilbert, L.I., Wilson, T.G., Song, Q., Li, S., 2009. Juvenile hormone
643 counteracts the bHLH-PAS transcription factors MET and GCE to prevent caspase-dependent
644 programmed cell death in *Drosophila*. *Development.* 136, 2015–2025.
645 https://doi.org/10.1242/dev.033712

646 Martín, D., Cruz, J., Franch-Marro, X., 2025, Hormonal control of insect metamorphosis. In:
647 Yamanaka N., Atkinson, P.W. (Eds.), Comprehensive Molecular Insect Science (2nd edition).
648 Elsevier Inc.

649 Mirth, C.K., Tang, H.Y., Makohon-Moore, S.C., Salhadar, S., Gokhale, R.H., Warner, R.D.,
650 Koyama, T., Riddiford, L.M., Shingleton, A.W., 2014. Juvenile hormone regulates body size and
651 perturbs insulin signaling in *Drosophila*. *Proc. Natl. Acad. Sci. U.S.A.* 111, 7018–7023.
652 https://doi.org/10.1073/pnas.1313058111

653 Moshitzky, P., Applebaum S.W., 1995. Pathway and regulation of JHIII-bisepoxide biosynthesis
654 in adult *Drosophila melanogaster* corpus allatum. *Arch. Insect. Biochem. Physiol*. 30, 225–37.
655 https://doi.org/10.1002/arch.940300211

656 Nauen, R., Bass, C., Feyereisen, R., Vontas, J., 2022. The role of cytochrome P450s in insect
657 toxicology and resistance. *Annu. Rev. Entomol.* 67, 105–124. https://doi.org/10.1146/annurev-
658 ento-070621-061328

659 Niwa, R., Niimi, T., Honda, N., Yoshiyama, M., Itoyama, K., Kataoka, H., Shinoda, T., 2008.
660 Juvenile hormone acid O-methyltransferase in *Drosophila melanogaster*. *Insect Biochem. Mol.*
661 *Biol*. 38, 714–20. https://doi.org/10.1016/j.ibmb.2008.04.003

662 Niwa, R., Niwa, Y.S., 2025. Molecular mechanisms of ecdysteroid biosynthesis. In: Yamanaka
663 N., Atkinson, P.W. (Eds.), Comprehensive Molecular Insect Science (2nd edition). Elsevier Inc.

664 Noriega, F.G., 2014. Juvenile hormone biosynthesis in insects: what is new, what do we know,
665 and what questions remain? *Int. Sch. Res. Notices.* 967361. https://doi.org/10.1155/2014/967361

666 Ohhara, Y., Kobayashi, S., Yamakawa-Kobayashi, K., Yamanaka, N., 2018. Adult-specific
667 insulin-producing neurons in *Drosophila melanogaster*. *J. Comp. Neurol.* 526, 1351–1367.
668 https://doi.org/10.1002/cne.24410

669 Okamoto, N., Viswanatha, R., Bittar, R., Li Z., Haga-Yamanaka, S., Perrimon, N., Yamanaka,
670 N., 2018. A membrane transporter is required for steroid hormone uptake in *Drosophila*. *Dev.*
671 *Cell.* 47, 294–305.e7. https://doi.org/10.1016/j.devcel.2018.09.012

672 Öztürk-Çolak, A., Marygold, S.J., Antonazzo, G., Attrill, H., Goutte-Gattat, D., Jenkins, V.K.,
673 Matthews, B.B., Millburn, G., Dos Santos, G., Tabone, C.J., 2024. FlyBase: updates to the
674 *Drosophila* genes and genomes database. *Genetics.* 227, iyad211.
675 https://doi.org/10.1093/genetics/iyad211

676 Rahman, M.M., Franch-Marro, X., Maestro, J.L., Martin, D., Casali A., 2017. Local juvenile
677 hormone activity regulates gut homeostasis and tumor growth in adult *Drosophila*. *Sci. Rep.* 7,
678 11677. https://doi.org/10.1038/s41598-017-11199-9

679 Ramirez, C.E., Nouzova, M., Michalkova, V., Fernandez-Lima, F., Noriega, F.G., 2020.
680 Common structural features facilitate the simultaneous identification and quantification of the
681 five most common juvenile hormones by liquid chromatography–tandem mass spectrometry.
682 *Insect Biochem. Mol. Biol.* 116, 103287. https://doi.org/10.1016/j.ibmb.2019.103287

683 Reiff, T., Jacobson, J., Cognigni, P., Antonello, Z., Ballesta, E., Tan, K.J., Yew, J.Y.,
684 Dominguez, M., Miguel-Aliaga, I., 2015. Endocrine remodelling of the adult intestine sustains
685 reproduction in *Drosophila*. *Elife.* e06930. https://doi.org/10.7554/eLife.06930

686 Ren, Q., Awasaki, T., Wang, Y.C., Huang, Y.F., Lee, T., 2018. Lineage-guided Notch-dependent
687 gliogenesis by *Drosophila* multipotent progenitors. *Development.* 145, dev160127.
688 https://doi.org/10.1242/dev.160127

689 Richard, D.S., Applebaum, S.W., Sliter, T.J., Baker, F.C., Schooley, D.A., Reuter, C.C.,
690 Henrich, V.C., Gilbert, L.I., 1989. Juvenile hormone bisepoxide biosynthesis in vitro by the ring
691 gland of *Drosophila melanogaster*: a putative juvenile hormone in the higher Diptera. *Proc. Natl.*
692 *Acad. Sci. U.S.A.* 86, 1421–1425. https://doi.org/10.1073/pnas.86.4.1421

693 Riddiford, L.M., Truman, J.W., Mirth, C.K., Shen, Y.C., 2010. A role for juvenile hormone in
694 the prepupal development of *Drosophila melanogaster*. *Development.* 137, 1117–1126.
695 https://doi.org/10.1242/dev.037218

696 Riddiford, L.M., 2020. *Rhodnius*, golden oil, and Met: a history of juvenile hormone research.
697 *Front. Cell Dev. Biol.* 8, 679. https://doi.org/10.3389/fcell.2020.00679

698 Rogers, M.F., Marshall, O.J., Secombe, J., 2023. KDM5-mediated activation of genes required
699 for mitochondrial biology is necessary for viability in *Drosophila*. *Development.* 150,
700 dev202024. https://doi.org/10.1242/dev.202024

701 Santos, C.G., Humann, F.C., Hartfelder, K., 2019. Juvenile hormone signaling in insect
702 oogenesis. *Curr. Opin. Insect Sci.* 31, 43–48. https://doi.org/10.1016/j.cois.2018.07.010

703 Sarro, E., Sun, P., Mauck, K., Rodriguez-Arellano, D., Yamanaka, N., Woodard, S.H., 2021. An
704 organizing feature of bumble bee life history: worker emergence promotes queen reproduction

705 and survival in young nests. *Conserv. Physiol.* 9, coab047.
706 https://doi.org/10.1093/conphys/coab047

707 Sayers, E.W., Bolton, E.E., Brister, J.R., Canese, K., Chan, J., Comeau, D.C. et al. 2022.
708 Database resources of the national center for biotechnology information. *Nucleic Acids Res.* 50,
709 D20–D26. https://doi.org/10.1093/nar/gkab1112

710 Shianiou, G., Teloni, S., Apidianakis, Y., 2023. Intestinal immune deficiency and juvenile
711 hormone signaling mediate a metabolic trade-off in adult *Drosophila* females. *Metabolites.* 13,
712 340. https://doi.org/10.3390/metabo13030340

713 Shinoda, T., Itoyama, K., 2003. Juvenile hormone acid methyltransferase: a key regulatory
714 enzyme for insect metamorphosis. *Proc. Natl. Acad. Sci. U.S.A.* 100, 11986–11991.
715 https://doi.org/10.1073/pnas.2134232100

716 Sliter, T.J., Sedlak, B.J., Baker, F.C., Schooley, D.A., 1987. Juvenile hormone in *Drosophila*
717 *melanogaster*: identification and titer determination during development. *Insect Biochem.* 17,
718 161–165. https://doi.org/10.1016/0020-1790(87)90156-9

719 Smykal, V., Dolezel, D., 2023. Evolution of proteins involved in the final steps of juvenile
720 hormone synthesis. *J. Insect Physiol.* 145, 104487.
721 https://doi.org/10.1016/j.jinsphys.2023.104487

722 Sugime, Y., Watanabe, D., Yasuno, Y., Shinada, T., Miura, T., Tanaka, N.K., 2017.
723 Upregulation of juvenile hormone titers in female *Drosophila melanogaster* through mating

724 experiences and host food occupied by eggs and larvae. *Zoolog. Sci.* 34, 52–57.
725 https://doi.org/10.2108/zs160150

726 Touhara, K., Bonning, B.C., Hammock, B.D., Prestwich, G.D., 1995. Action of juvenile
727 hormone esterase on the JH–JH binding protein complex: an in vitro model of JH metabolism in
728 a caterpillar. *Insect Biochem. Mol. Biol.* 25, 727–734. https://doi.org/10.1016/0965-
729 1748(95)00012-K

730 Trowell, S.C., Hines, E.R., Herlt, A.J., Rickards, R.W. 1994. Characterization of a juvenile
731 hormone binding lipophorin from the blowfly *Lucilia cuprina*. *Comp. Biochem. Physiol. B*
732 *Biochem. Mol. Biol.* 109, 339–357. https://doi.org/10.1016/0305-0491(94)90018-3

733 Wen, D., Rivera-Perez, C., Abdou, M., Jia, Q., He, Q., Liu, X., Zyaan, O., Xu, J., Bendena,
734 W.G., Tobe, S.S., Noriega, F.G., Palli, S.R., Wang, J., Li, S. 2015. Methyl farnesoate plays a
735 dual role in regulating *Drosophila* metamorphosis. *PLoS Genet.* 11, e1005038.
736 https://doi.org/10.1371/journal.pgen.1005038

737 Wijesekera, T.P., Saurabh, S., Dauwalder, B. 2016. Juvenile hormone is required in adult males
738 for *Drosophila* courtship. *PLoS One.* 11, e0151912.
739 https://doi.org/10.1371/journal.pone.0151912

740 Wilson, T.G., Ashok, M. 1998. Insecticide resistance resulting from an absence of target-site
741 gene product. *Proc. Natl. Acad. Sci. U.S.A.* 95, 14040–14044.
742 https://doi.org/10.1073/pnas.95.24.14040

743 Wilson, T.G., DeMoor, S., Lei, J. 2003. Juvenile hormone involvement in *Drosophila*
744 *melanogaster* male reproduction as suggested by the *Methoprene-tolerant* mutant phenotype.
745 *Insect Biochem. Mol. Biol.* 33, 1167–1175. https://doi.org/10.1016/j.ibmb.2003.06.007

746 Wu, B., Ma, L., Zhang, E., Du, J., Liu, S., Price, J., Li, S., Zhao, Z. 2018. Sexual dimorphism of
747 sleep regulated by juvenile hormone signaling in *Drosophila*. *PLoS Genet.* 14, e1007318.
748 https://doi.org/10.1371/journal.pgen.1007318

749 Yamamoto, R., Bai, H., Dolezal, A.G., Amdam, G., Tatar, M. 2013. Juvenile hormone regulation
750 of *Drosophila* aging. *BMC Biol.* 11, 85. https://doi.org/10.1186/1741-7007-11-85

751 Zhang, X., Li, S., Liu, S. 2022. Juvenile Hormone Studies in *Drosophila melanogaster*. *Front.*
752 *Physiol.* 12, 785320. https://doi.org/10.3389/fphys.2021.785320

753

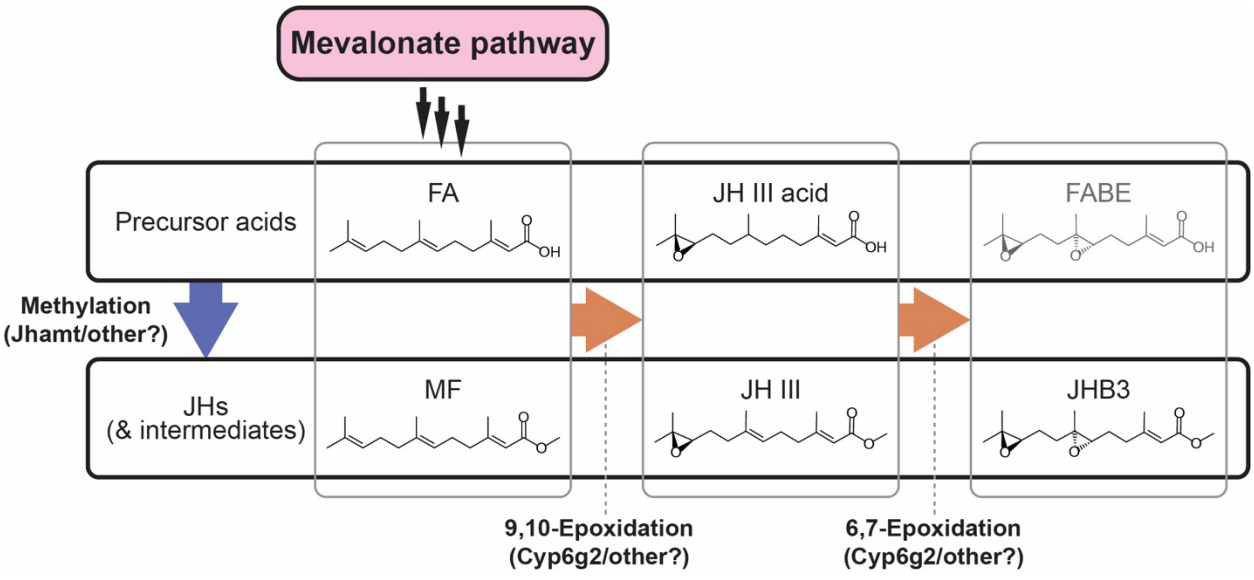

Figure 1. Last steps of the JH biosynthetic pathway in *Drosophila melanogaster*. Farnesoic acid (FA) is converted into juvenile hormone III (JH III) and JH-bisepoxide (JHB3) in the corpus allatum. Cyp6g2 predominantly epoxidizes FA into JH III acid, rather than methyl farnesoate (MF) into JH III (Jia et al., 2024). Jhamt converts both FA and JH III acid into MF and JH III, respectively (Niwa et al., 2008). Although FA bisepoxide (FABE) has been hypothesized as an intermediate of JHB3 synthesis (Moshitzky and Applebaum, 1995), it has not been detected in *D. melanogaster*.

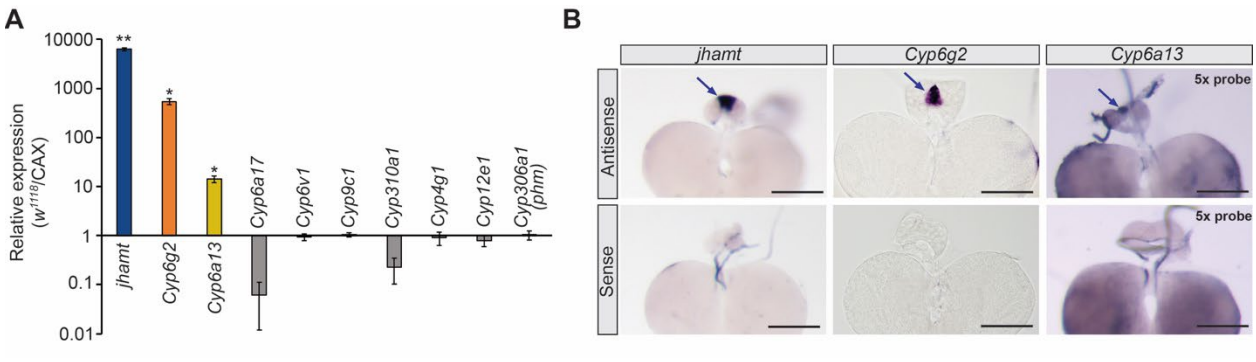

Figure 2. Cytochrome P450 genes highly expressed in the larval CA.

(**A**) Relative gene expression levels in the ring gland (RG) of control (w^{1118}) as compared to corpus allatum (CA)-ablated (CAX) larvae. *jhamt* and cytochrome P450 genes highly expressed in the RG of wandering larvae were quantified. High relative expression levels indicate CA-specific expression. Expression levels were normalized to a reference gene, *rp49*, in the same cDNA samples. Values are the means ± standard error ($n = 3$). *$p < 0.05$, **$p < 0.01$ (Student's *t*-test). (**B**) *In situ* hybridization of *jhamt*, *Cyp6g2*, and *Cyp6a13* in the larval RG. Due to the lower expression of *Cyp6a13*, five times more RNA probe was used. CA is indicated by arrows. Scale bars: 100 µm.

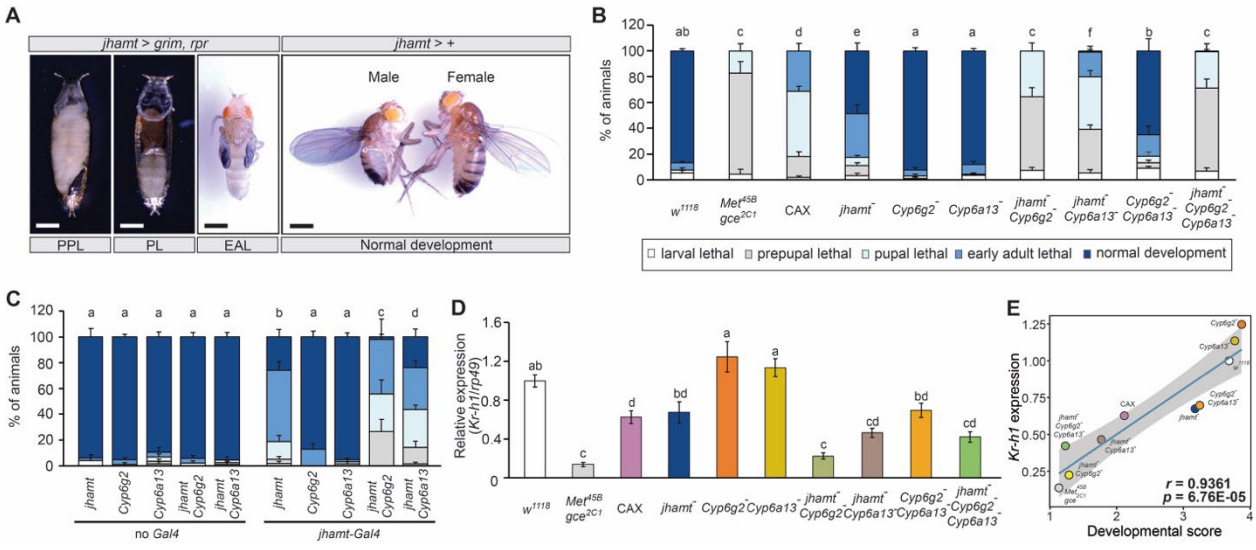

774

775 **Figure 3. Lethal phenotypes of CA-ablated flies and JH-related mutants.**

776 (**A**) Representative images of the lethal phenotypes of corpus allatum (CA)-ablated (CAX) flies
777 induced by *jhamt-LexA*-driven expression of *grim* and *reaper* (*rpr*). CAX flies died at different
778 stages of metamorphosis. (**B**) Developmental lethality observed in CAX flies and homozygous
779 mutants of JH-related genes. Receptor double mutants and combined mutants of *jhamt* with
780 *Cyp6g2* or *Cyp6a13* exhibited severe lethality. Values are the means ± standard error. $n = 3$
781 (Met^{45B}, gce^{2C1}) or $n = 6$ (other mutants). Different letters above the bars indicate statistically
782 significant differences ($p < 0.05$) between groups (Chi-square test with Bonferroni correction).
783 (**C**) CA-specific knockdown of enzymes induced by *jhamt-Gal4*. Combined knockdown of *jhamt*
784 with *Cyp6g2* or *Cyp6a13* exhibited severe lethality. Values are the means ± standard error ($n =$
785 3–4). Different letters above the bars indicate statistically significant differences ($p < 0.05$, Chi-
786 square test with Bonferroni correction). (**D**) Relative expression levels of *Kruppel homolog 1*
787 (*Kr-h1*) in CAX and mutant flies at 0 h after puparium formation. Expression levels were
788 normalized to a reference gene, *rp49*, in the same cDNA samples. Flies with severe lethality tend
789 to show lower expression levels. Values are the means ± standard error ($n = 4$–7). Different
790 letters above the bars indicate statistically significant differences ($p < 0.05$, Tukey's honestly

791 significant difference test). (**E**) Correlation between developmental lethality and *Kr-h1*

792 expression levels at 0 hour after puparium formation. Developmental scores were calculated

793 based on lethal stages. A strong correlation ($r = 0.9361$) was observed between lethality and *Kr-*

794 *h1* expression levels across various genotypes.

795

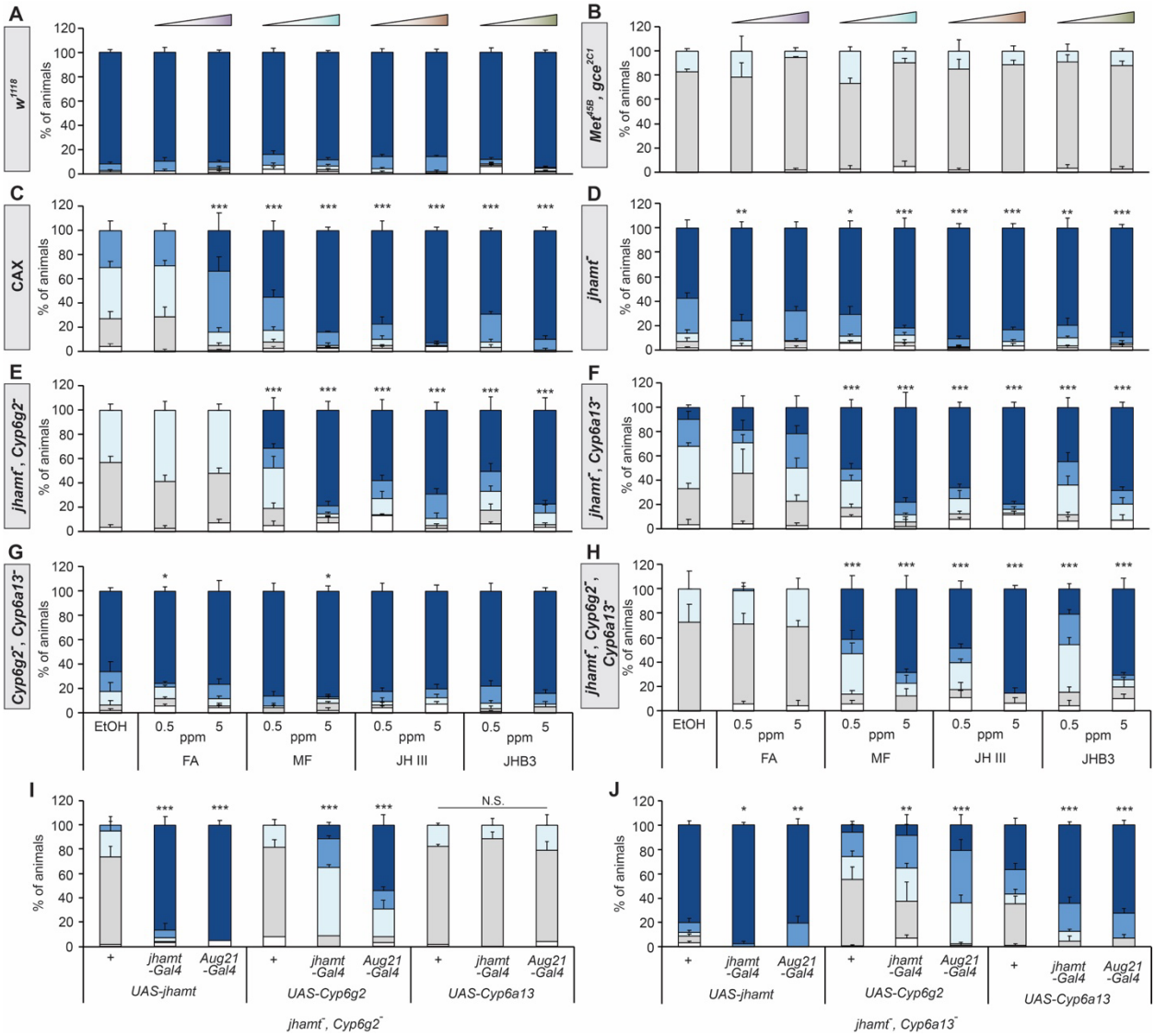

Figure 4. Rescue of CA-ablated flies and JH-related mutants.

(**A-H**) Rescue of developmental defects observed in control (w^{1118}), corpus allatum (CA)-ablated (CAX) flies, and homozygous mutants of JH-related genes by application of farnesoic acid (FA), methyl farnesoate (MF), juvenile hormone III (JH III), or juvenile hormone III bisepoxide (JHB3). Larvae were transferred onto the diet containing 0.5 or 5 ppm of one of the sesquiterpenoids at 48 hours after hatching and raised until eclosion. MF, JH III, and JHB3 rescued lethality of most genotypes, whereas FA had little effect. Values are the means ± standard error (n = 3–6). *$p < 0.05$, **$p < 0.01$, ***$p < 0.001$ (Chi-square test with Bonferroni

805 correction *vs* application of the solvent (EtOH) alone). (**I, J**) Rescue of *jhamt*, *Cyp6g2* (I) or

806 *jhamt*, *Cyp6a13* (J) double mutants by CA-specific overexpression of *jhamt*, *Cyp6g2*, or

807 *Cyp6a13*. *Cyp6g2* overexpression partially rescued *jhamt*, *Cyp6a13* double mutants, but

808 *Cyp6a13* overexpression did not rescue *jhamt*, *Cyp6g2* double mutants. Values are the means ±

809 standard error (n = 3–6). **$p < 0.01$, ***$p < 0.001$ (Chi-square test with Bonferroni correction *vs*

810 control flies without a *Gal4* driver). N.S., not significant ($p > 0.05$).

811

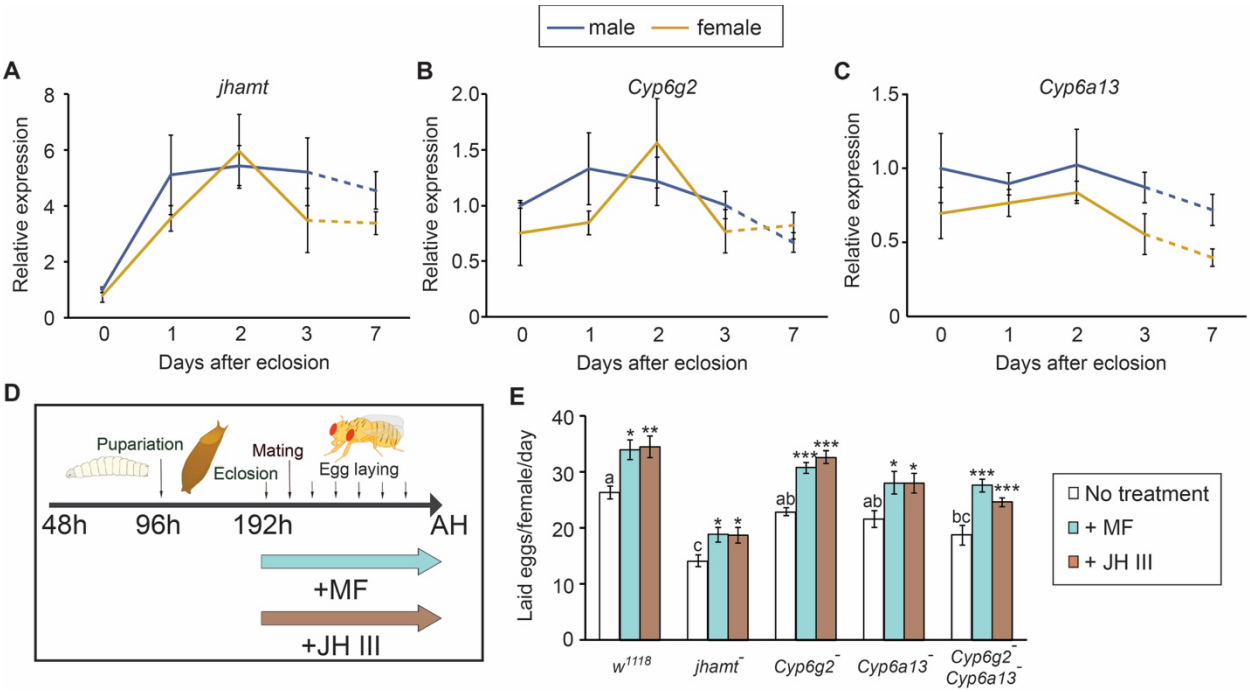

Figure 5. Contributions of the CA-expressed enzymes to reproduction.

(**A**–**C**) Changes in gene expression of *jhamt* (A), *Cyp6g2* (B), and *Cyp6a13* (C) in the corpus allatum/corpora cardiaca complex of the adults expressing *jhamt-LexA*-driven *LexAop-mCD8::GFP*. Expression levels were normalized to levels at day 0 after eclosion (within 6 hours). Values are the means ± standard error (n = 3–4). (**D**) Schematic diagram of the fecundity assay. Mutants were reared normally until eclosion. Eclosed adults were then maintained with or without methyl farnesoate (MF) or juvenile hormone III (JH III). Mutant females were mated with w^{1118} males 24 hours after eclosion. The number of eggs laid was counted every 24 hours from 3 to 7 days after eclosion. *Drosophila* illustrations were obtained from TogoTV (© 2016 DBCLS TogoTV, CC-BY-4.0 https://creativecommons.org/licenses/by/4.0/deed.ja). (**E**) Number of eggs laid by the mutant females. The numbers of eggs laid by untreated females were compared across genotypes using Tukey's honestly significant difference test. Different letters above the bars indicate statistically significant differences among different genotypes ($p < 0.05$). The numbers of eggs laid by MF- or JH III-treated females were compared to that of untreated

827 females of the same genotype using Dunnett's test (*$p < 0.05$, **$p < 0.01$, ***$p < 0.001$). *jhamt*

828 mutant and *Cyp6g2*, *Cyp6a13* double mutant females laid significantly fewer eggs than w^{1118}

829 control. Sesquiterpenoid treatment enhanced egg production in all genotypes tested. Values are

830 the means ± standard error (n = 6–12).

831

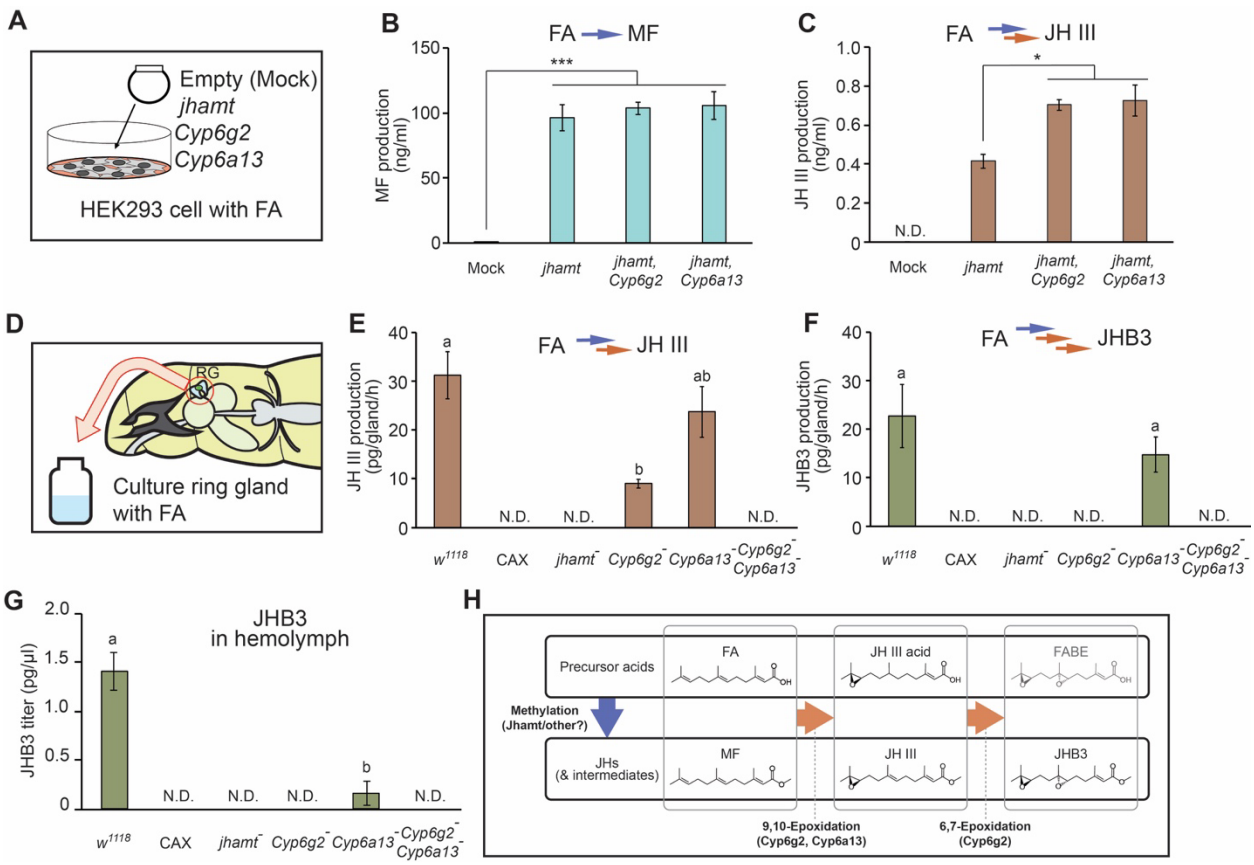

Figure 6. Functional analyses of the CA-expressed enzymes.

(**A**) Schematic diagram of the enzymatic conversion assay in HEK293 cells. (**B, C**) Conversion of farnesoic acid (FA) into methyl farnesoate (MF) (B) and juvenile hormone III (JH III) (C) in HEK293 cells ectopically expressing the CA-expressed enzymes. Jhamt catalyzes methylation, while Cyp6g2 and Cyp6a13 catalyze epoxidation to synthesize JH III. Values are the means ± standard error (n = 3–4). *$p < 0.05$, ***$p < 0.001$ (Tukey's honestly significant difference test). N.D., not detected. (**D**) Schematic diagram of *ex vivo* culture of the ring glands from wandering larvae. (**E, F**) Conversion of FA into JH III (E) and juvenile hormone III bisepoxide (JHB3) (F) in cultured ring glands. JH production in the *jhamt* mutant ring glands was drastically reduced. The *Cyp6g2* mutant ring glands produced only a small amount of JH III. While JH production in the *Cyp6a13* mutant ring glands was not significantly reduced, it was abolished in the *Cyp6g2*,

844 *Cyp6a13* double mutant ring glands. Different letters above the bars indicate significant
845 differences ($p < 0.05$, Tukey's honestly significant difference test). Values are the means ±
846 standard error ($n = 4$–12). N.D., not detected. (**G**) JHB3 titers in the hemolymph of wandering
847 larvae of control (w^{1118}), corpus allatum (CA)-ablated (CAX) flies, and the enzyme mutants. The
848 hemolymph JHB3 titer was significantly reduced in *Cyp6a13* mutant larvae, and it was
849 undetectable in CAX, *jhamt* mutant, *Cyp6g2* mutant, and *Cyp6g2*, *Cyp6a13* double mutant
850 larvae. MF and JH III were below detection limits. Different letters above the bars indicate
851 significant differences ($p < 0.05$, Tukey's honestly significant difference test). Values are the
852 means ± standard error ($n = 4$–7). N.D., not detected. (**H**) Proposed model of the JH biosynthetic
853 pathway in the *Drosophila* CA.